

# Analytical Considerations for Thin Concrete Overlays on Asphalt

JAMES W. MACK, LAWRENCE W. COLE, AND J. P. MOHSEN

An analytical study was undertaken to account for the performance of a thin concrete overlay on an asphalt concrete (AC) pavement built in Louisville, Kentucky, in September 1991. Initial investigations and theoretical studies based on conventional concrete theory indicated that the pavement should have failed after its first few loadings. However, this did not happen. After 11 months of use, with very heavy traffic (400 to 600 garbage trucks per day, 5½ days a week), the pavement has provided much better service than was anticipated, suggesting that a bond developed between the concrete overlay and underlying AC that greatly improved the pavement's performance. Some direction for future research is provided.

Concrete overlays on asphalt concrete (AC) pavements (whitotopping) have been successfully used as rehabilitation procedures for deteriorated AC pavements since 1944. In that year, an airfield at the U.S. Air Force Base in Offut, Nebraska, was successfully whitotopped. Since that time, many more whitotopping projects have been built throughout the United States and worldwide. Generally, these concrete overlays are a minimum of 127 mm (5.0 in.) thick and designed with conventional concrete pavement theory that characterizes the AC pavement as a stabilized base using Westergaard's modulus of subgrade reaction ( $k$ ).

To investigate the performance of a thin concrete overlay [less than 127 mm (5.0 in.) thick] on AC, the Portland Cement Association, the American Concrete Pavement Association, and other industry groups combined to build an experimental project in Louisville, Kentucky, in September 1991. The overlay was constructed on the Waste Management Corporation's Outer Loop Recycling and Disposal Facility access road. This site was chosen because of the high number of trucks that use the facility (400 to 600 trucks per day, 5½ days a week). The existing AC pavement was in relatively uniform condition with some minor surface distortions and mild rutting in the existing AC; however, there were no cracks or structural failures in the test sections. To obtain a uniform overlay thickness, the AC pavement was milled before the concrete overlay was placed. This milling left the AC surface with a rough surface. Initially, the milled surface was believed to be approximately 102 mm (4.0 in.) thick; however, later, it was found to be slightly less.

The experimental project consisted of two sections (Figure 1). The first section consisted of a 89-mm (3.5-in.) pavement cut into 1.83- × 1.83-m (6- × 6-ft) panels. The second section was a 51-mm (2.0-in.) pavement cut into 1.83-; × 1.83-m (6-

× 6-ft) panels and 0.61- × 0.61-m (2- × 2-ft) panels. The concrete was a high early-strength mixture with polypropylene fibers capable of obtaining a laboratory compressive strength of 27.59 MPa (4,000 lb/in.<sup>2</sup>) in 18 hr. Approximately 3 hr after concrete placement, the 1.83-m (6-ft) spaced control joints were sawed into the overlay. These joints were ¼ the pavement depth. In the 0.61-m (2-ft) panels, saw joints 25.4 mm (1.0 in.) deep were used to ensure that slab interaction would be minimal. None of these joints was sealed. Additional information on the construction of this project may be found elsewhere (1).

## ANALYTICAL INVESTIGATION

### Concrete and Subgrade Support Characterization

For analysis, the properties of the concrete and AC layers had to be determined. Concrete compression strengths were determined to be 23.6 MPa (3,422 lb/in.<sup>2</sup>) at 24 hr, 33.74 MPa (4,893 lb/in.<sup>2</sup>) at 36 hr, 35.32 MPa (5,122 lb/in.<sup>2</sup>) at 48 hr, 44.50 MPa (6,453 lb/in.<sup>2</sup>) at 7 days, and 51.07 MPa (7,405 lb/in.<sup>2</sup>) at 28 days per ASTM C39. Third-point beam flexural strengths were determined to be 5.23 MPa (759 lb/in.<sup>2</sup>) at 24 hr, 5.77 MPa (837 lb/in.<sup>2</sup>) at 36 hr, and 7.07 MPa (1,025 lb/in.<sup>2</sup>) at 28 days per ASTM C78. The modulus of elasticity for the concrete ( $E_c$ ) was determined by 34 473 MPa (5 million lb/in.<sup>2</sup>) using the 28-day compressive strength and the following American Concrete Institute (ACI) equation:

$$E_c = 4.73 \sqrt{f'_c} (\text{MPa}) \quad [E_c = 57,000 \sqrt{f'_c} (\text{lb/in.}^2)] \quad (1)$$

where  $f'_c$  is the compressive strength.

In addition to the concrete testing, falling weight deflectometer (FWD) measurements were taken on the AC after milling and on the concrete overlay 24 hr after construction. The backcalculation computer programs BISDEF (2) and ILLI-BACK (3) were used to characterize the AC pavement and subgrade support. These analyses determined the AC modulus of elasticity ( $E_{ac}$ ) to be 3447 MPa (500,000 lb/in.<sup>2</sup>), the  $k$  on top of the AC pavement to be 68.0 MPa/m (250 lb/in.<sup>2</sup>), and the subgrade modulus of elasticity ( $E_{sg}$ ) to be in the range of 186.2 to 206.9 MPa (27,000 to 30,000 lb/in.<sup>2</sup>).

### Westergaard Analysis To Determine Stresses and Deflections

An initial analytical investigation of the pavement sections started shortly after the pavement was open to traffic. Most

J. W. Mack and L. W. Cole, American Concrete Pavement Association, 3800 N. Wilke Road, Suite 490, Arlington Heights, Ill. 60004.  
J. P. Mohsen, University of Louisville, Louisville, KY. 40208.

**Mix Design**

Type 1 Cement	474.4 kg/m <sup>3</sup>
Coarse Aggregate (#8 crushed limestone)	10688 kg/m <sup>3</sup>
Fine Aggregate (Natural sand)	948.2 kg/m <sup>3</sup>
Air Content	4%-6%
High Range Water Reducer (ASTM C-494, Type F)	0.9128 ml/100 kg cement
Polypropylene Fibers (Graded, fibrillated)	1.78 kg/m <sup>3</sup>

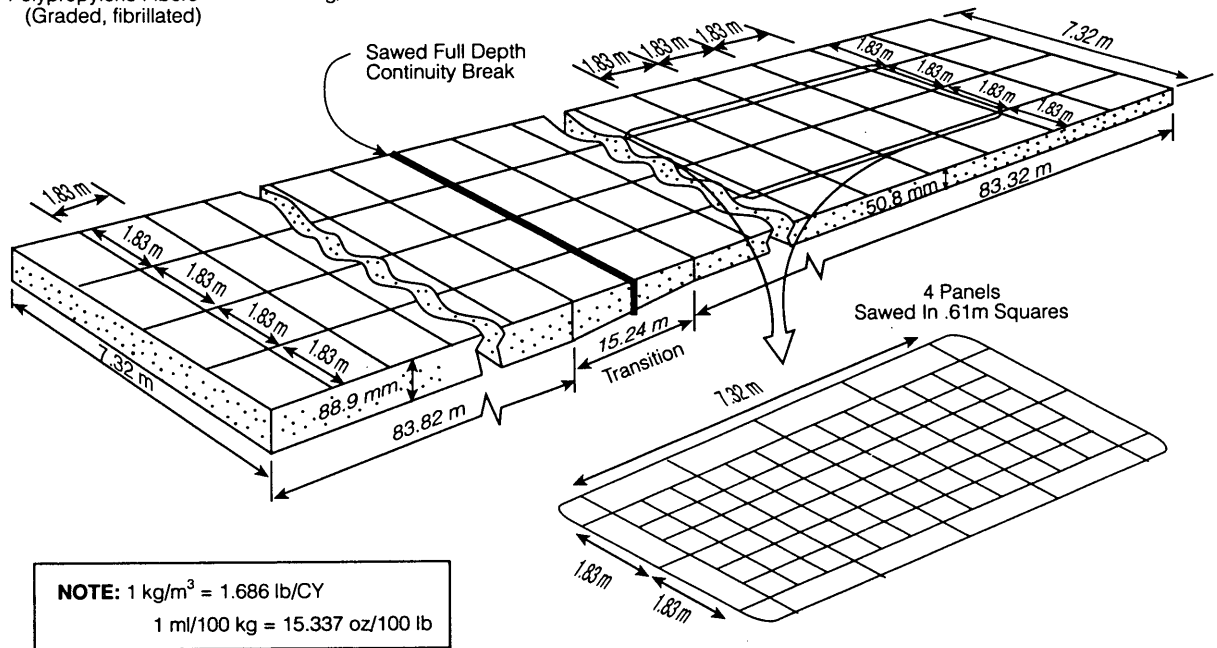


**FIGURE 1** Layout of experimental section.

experiment observers assumed that the pavement would crack shortly after opening to traffic. However, after 4 weeks of truck loading with approximately 43,000 80-kN (18-kip) equivalent single-axle loads (ESALs), only 6 percent of the pavement showed visible distress, with all of the distresses concentrated in the 1.83-m (6-ft) panels. Corner cracking was the primary distress mode. Less than 0.6 percent of the slabs exhibited transverse cracking. The 0.61-m (2-ft) panels had no signs of cracking of any type (4).

The initial analysis used the following Westergaard equations (5) to calculate interior, edge, and corner stresses and deflections caused by a single wheel load.

Maximum stress (lb/in.<sup>2</sup>):

$$\begin{aligned}
 \text{[Edge stress} &= 3(1 + \mu)P/[\pi(3 + \mu)h^2] \\
 & * [\ln(Eh^3)/(100ka^4) \\
 & + 1.84 - 4\mu/3 + (1 - \mu)/2 \\
 & + 1.18(1 + 2\mu)(a/l)] \quad (2)
 \end{aligned}$$

$$\begin{aligned}
 \text{Interior stress} &= 3P(1 + \mu)/(2\pi h^2) \\
 & * [\ln(2l/b) + 0.5 - \gamma] \\
 & + 3P(1 + \mu)/(64h^2) * (a/l)^2 \quad (3)
 \end{aligned}$$

$$\text{Corner stress} = 3P/(h^2)[1 - (a\sqrt{2l})^{0.6}] \quad (4)$$

Maximum deflections (in.):

$$\begin{aligned}
 \text{Edge deflection} &= P(2 + 1.2\mu)^{0.5}/[(Ek h^3)^{0.5}] \\
 & * [1 - (0.76 + 0.4\mu)(a/l)] \quad (5)
 \end{aligned}$$

Interior deflection

$$= P/(8kF) * [1 + 0.5\pi[\ln(a/2l) + \gamma - 5/4] * (a/l)^2] \quad (6)$$

$$\text{Corner deflection} = [1.1 - 1.24(a/l)]P/(kF) \quad (7)$$

where

- $\mu$  = Poisson's ratio;
- $P$  = total load [N (lb)];
- $h$  = thickness [mm (in.)];
- $l$  = radius of relative stiffness [mm (in.)];
- $l^4 = E_c h^3 / [12(1 - \mu^2)k]$ ;
- $b = a$  if  $a > 1.724h$  (which is true in this case);
- $b = -.0675h + (1.6a^2 + h^2)$  if  $a < 1.724h$ ;
- $a$  = equivalent radius of a plate with semiaxis at  $x$  and  $y$ ,
- $r = (x^2 + y^2)/2$ ;
- $\gamma$  = Euler's constant = 0.5772156649;
- $E_c$  = elastic modulus of concrete, MPa (lb/in.<sup>2</sup>); and
- $k$  = modulus of subgrade reaction, MPa/m (lb/in.<sup>2</sup>).

This analysis found the maximum stress and deflection in the 51-mm (2.0-in.) overlay to be 18.006 MPa (2,611 lb/in.<sup>2</sup>) and 3.69 mm (0.1453 in.), respectively. For the 89-mm (3.5-in.) overlay, the maximum stress and deflection were 8.160 MPa (1,183 lb/in.<sup>2</sup>) and 2.19 mm (0.0863), respectively. These maximum calculated stresses for single-wheel load were well above the 36-hr flexural strength of the pavement when it was opened to traffic and indicated that the pavement should have cracked in the transverse direction.

### Finite Element Analysis

Because the Westergaard analysis failed to explain the pavement's performance, an additional analysis was performed using finite element procedures with the finite element computer program ILLI-SLAB (6,7). ILLI-SLAB calculates deflections and stresses in jointed slabs-on-grade pavements, with and without load transfer, for various subgrade support conditions. For this analysis, the pavement was modeled as a one-layer and two-layer system on a Winkler foundation. The  $k$  value for the one-layer system was set to 68.0 MPa/m (250 lb/in.<sup>2</sup>/in.), the  $k$  value on top of the AC. For the two-layer system,  $k$  was altered between 27.2, 40.8, and 54.4 MPa/m (100, 150, and 200 lb/in.<sup>2</sup>/in.) and  $E_{ac}$  was set to 3,447 MPa (500,000 lb/in.<sup>2</sup>). The load was modeled as a dual tire load on 279- × 228-mm (11- × 9-in.) wheels. This roughly corresponds to a tire aspect ratio of 0.8. The modeled load was 36.0 kN (8,100 lb) per tire, which was the average test load used at the Louisville experimental project. The majority of the analysis work was done on the 1.83- × 1.83-m (6- × 6-ft) slabs, which were modeled as single slabs. Only one slab could be modeled at a time because of the mesh fineness required by ILLI-SLAB to get accurate values for stresses and deflections. Analysis work was also done on the 0.61- × 0.61-m (2- × 2-ft) slabs. These slabs were modeled with the same mesh patterns used for the 1.83- × 1.83-m (6- × 6-ft) slabs, except that joints were placed at 610 mm (24 in.) and 1220 mm (48 in.), which created a multislabs model with three slabs extending in both the  $x$  and  $y$  directions.

### Single-Layer Analysis

The single-layer analysis model for the 51-mm (2.0-in.) and 89-mm (3.5-in.) pavements used the stiff subgrade [ $k = 68.0$  MPa/m (250 lb/in.<sup>2</sup>/in.)] determined from the FWD testing and the concrete material properties ( $E_c$ ) described earlier. This analysis calculated a maximum stress of 20.182 MPa (2,926 lb/in.<sup>2</sup>) and a maximum deflection of 6.01 mm (0.2366 in.) for the 51-mm overlay and 10.104 MPa (1,465 lb/in.<sup>2</sup>) and 3.78 mm (0.1567 in.), respectively, for the 89-mm (3.5-in.) pavement. Although these values generally were in close agreement with the values obtained from the single layer Westergaard analysis, they still failed to explain the pavements' behavior.

### Two-Layer Analysis

The two-layer analysis had the pavement modeled as concrete over a 102-mm (4-in.) AC pavement on top of a subgrade

with  $k$  values of 27.2, 40.8, and 54.4 MPa/m (100, 150, and 200 lb/in.<sup>2</sup>/in.). These  $k$  values were chosen as a representative range of values underneath the AC layer. Because the  $k$  on top of the AC was 68.0 MPa/m (250 lb/in.<sup>2</sup>/in.), it was deduced that the  $k$  underneath it had to be some lesser value. The AC layer was modeled with an  $E_{ac}$  of 3447 MPa (500,000 lb/in.<sup>2</sup>) and a Poisson's ratio of 0.3. Interface conditions were modeled as bonded and unbonded. The loading conditions modeled were at the interior, corner, and edges of the slab. The analysis results for maximum calculated stresses and deflections are presented in Figures 2 and 3.

Figure 2 indicates the significant effect of bond between the concrete overlay and AC pavement on the maximum calculated stresses in the concrete overlay. By bonding the upper concrete layer to the lower AC layer, much of the load is transferred down into the pavement structure, keeping the stresses in the concrete well within acceptable limits. Figure 2 also shows the relative insensitivity of the calculated stresses to the various subgrade support conditions or  $k$  values. This is opposite of what happens with the deflections for the bonded and unbonded systems. As indicated in Figure 3, deflection is somewhat insensitive to the bonding conditions between the layers and more sensitive to the subgrade  $k$  value. Although bond does decrease the deflections, the  $k$  value of the subgrade has a much larger impact on decreasing the deflections.

It is important to note the magnitude of the deflections obtained for these pavements. Most concrete pavements usually do not deflect more than about 0.8 mm (0.03 in.). However, for both the bonded and unbonded thin concrete overlays on the soft subgrade [ $k = 27.15$  MPa/m (100 lb/in.<sup>2</sup>/in.)], the calculated deflections are much higher than this. For corners, where deflection is the highest, the deflection may be over 5 mm (0.2 in.) for both conditions. Such high deflections on soft subgrades must be considered in the design of such pavement structures because they may lead to permanent subgrade deformations and early failures.

One unexpected anomaly is found when comparing the stress values of the bonded 51-mm (2.0-in.) overlay to the stresses of the bonded 89-mm (3.5-in.) overlay. As shown in Figure 2, the calculated bonded stresses in the 51-mm (2.0-in.) concrete pavement are actually lower than the stresses in the bonded 89-mm (3.5-in.) pavement. This is the opposite

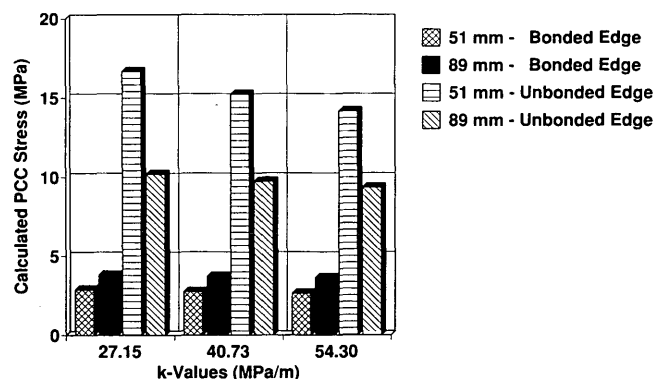


FIGURE 2 Maximum calculated edge stresses.

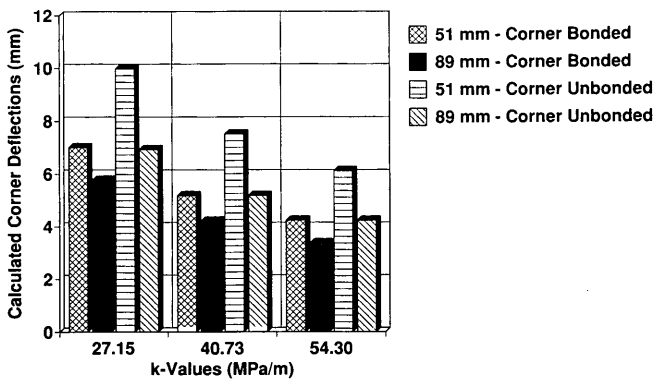


FIGURE 3 Maximum calculated corner deflections.

of what happens in the unbonded systems and goes against conventional concrete pavement theory.

This phenomenon can be explained by examining the location of the neutral axis with respect to the bottom of the concrete slab. Figure 4 shows stress diagrams for both the 51-mm (2.0-in.) and 89-mm (3.5-in.) pavement in the bonded condition. This figure shows that although the neutral axis stays in the bottom half of the concrete slab, its location from the bottom of the slab increases as the slab gets thicker. As the neutral axis gets farther away from the bottom, the flexural stress at the bottom of the concrete increases as more of the load is carried by the concrete slab. Also shown in Figures 4 and 5 is the decrease in the AC layer stresses caused by an upward shift of the neutral axis. Basically, in the 51-mm (2.0-in.) pavement, more load is carried by the lower layer, as shown by the higher AC stress value. As the concrete thickens to 89 mm (3.5 in.), the neutral axis shifts up, more load is absorbed by the concrete, and the stresses in the AC layer decrease.

Both the 51-mm (2.0-in.) and the 89-mm (3.5-in.) systems carry the same total load; however, the shifting of the neutral axis changes the amount of the load carried by each individual layer. As the neutral axis gets lower, more of the total load is carried in the AC layer and less by the concrete, and as the neutral axis gets higher, more of the total load is carried by the concrete and less by the AC. Eventually, as the concrete overlay thickness increases, the effect of shifting the neutral axis is offset by the overlay thickness itself; that is, the stresses will start to decrease as the thickness increases.

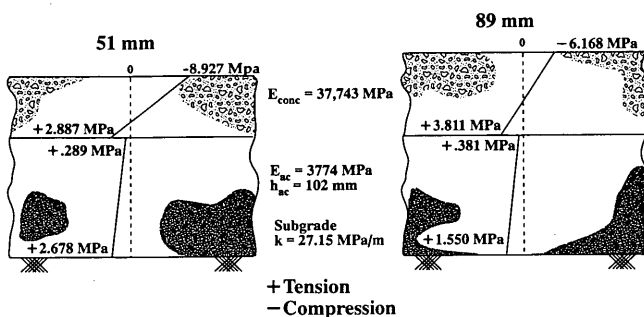


FIGURE 4 Stress distribution for bonded overlay.

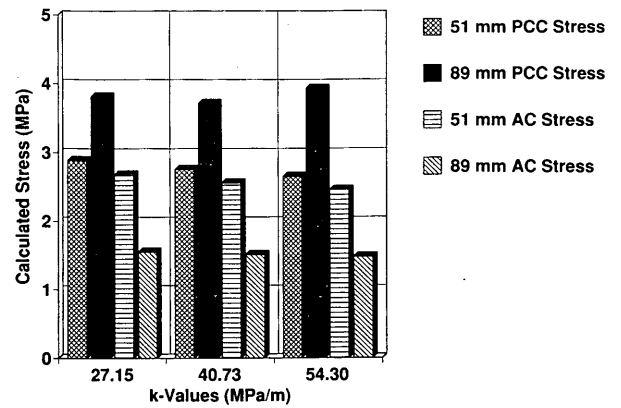


FIGURE 5 Calculated stresses in bottom of PCC and AC layers for bonded condition at edge loading.

This phenomenon is indicated in Figure 6, in which a 127.0-mm (5.0-in.) pavement section, using the same mesh, material properties, and loading conditions as the 51-mm (2.0-in.) and 89-mm (3.5-in.) pavements, was evaluated using ILLI-SLAB. As shown, the calculated stresses in the 127.0-mm (5.0-in.) overlay are lower than the stresses from the 89-mm (3.5-in.) overlay because the upward shift of the neutral axis is offset by the thickness.

Conceptually, this phenomenon is shown in Figure 7 for a given AC thickness. As the location of the neutral axis moves further from the bottom of the slab, or to the right, the stresses at the bottom of the concrete increase because of the shifting of the load from the AC to the concrete. Conversely, as the concrete overlay thickness increases, the stresses decrease because of the increase of the load-carrying capacity of the slab. At the point where the two lines cross, the neutral axis is high enough and the slab thickness is thin enough to produce maximum stresses in the slab bottom. An increase in concrete overlay thickness will lower the stresses associated with concrete slab thickness, and a decrease in thickness will decrease the stresses associated with the lowering of the neutral axis.

Although only one AC thickness value was used at Louisville, the effect of the underlying AC layer thickness on the location of the neutral axis was also evaluated. As the AC layer thickens, it becomes stiffer, and the neutral axis shifts

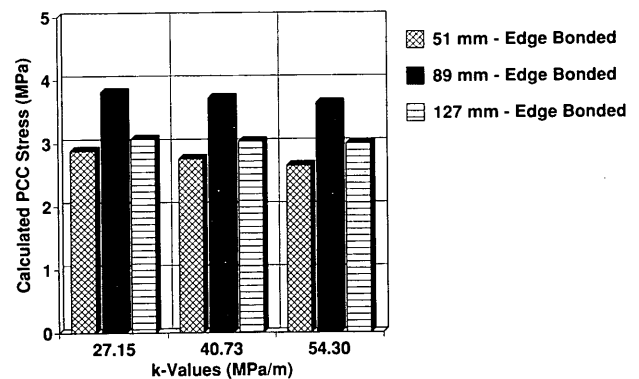
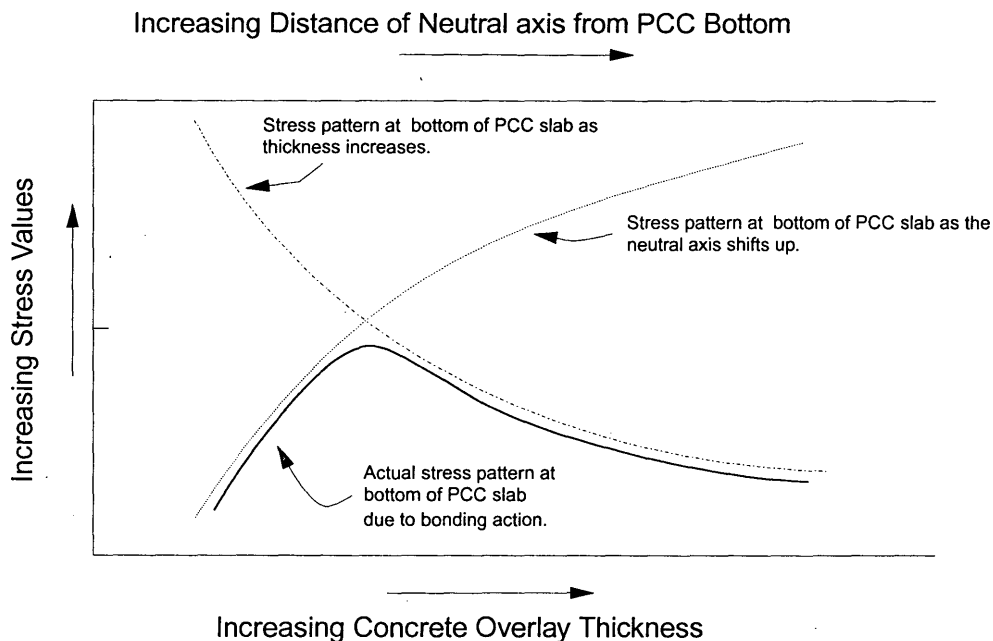


FIGURE 6 Calculated edge stresses for various PCC thicknesses.



**FIGURE 7** Conceptual stress pattern at PCC slab bottom caused by location of neutral axis and thickness of slab for a bonded system with a constant AC thickness.

down. Likewise, as the AC layer gets thinner, it carries less of the applied load and the neutral axis shifts up. A diagram similar to that in Figure 7 could be developed for constant concrete thickness that would show when the neutral axis was at its most critical location for various AC thicknesses. Figures 8 and 9 show how the concrete and AC stresses are affected by the concrete overlay and AC thicknesses.

Theoretically, the effect of concrete and AC thickness can be explained by the stiffness or flexural rigidity of the two layers. Flexural rigidity of a layer ( $D$ ) is defined as

$$D = \frac{Eh^3}{12(1 - \mu^2)} \quad (8)$$

where

- $E$  = modulus of elasticity,
- $h$  = thickness, and
- $\mu$  = Poisson's ratio.

Simply put, as the rigidity of a layer increases, the load-carrying capacity of the layer increases. In a bonded system, changing the rigidity of a single layer by changing the thickness changes the rigidity of the entire system and shifts the neutral axis. Note that the layer with the larger rigidity value will take the larger portion of the load. As the concrete slab thickness increases, the effects of the AC thickness increase become less pronounced. Although it has not been tested here, it is believed that changes in the modulus values will have a similar, but smaller, effect. This is a very critical concept because the neutral axis will be in a different location for every concrete and AC modulus value and every concrete and AC thickness. If a pavement happens to be built at a thickness that is near the intersection of the two lines in Figure 7, it will fail earlier than if it was built thicker or thinner.

Expanding this rigidity concept, it would be possible to describe any portland cement concrete (PCC)/AC system as an equivalent single layer with an equivalent modulus and

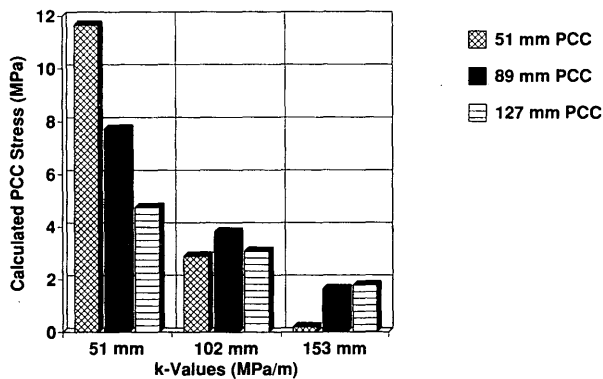


**FIGURE 8** Calculated PCC stresses for various AC and PCC thicknesses.

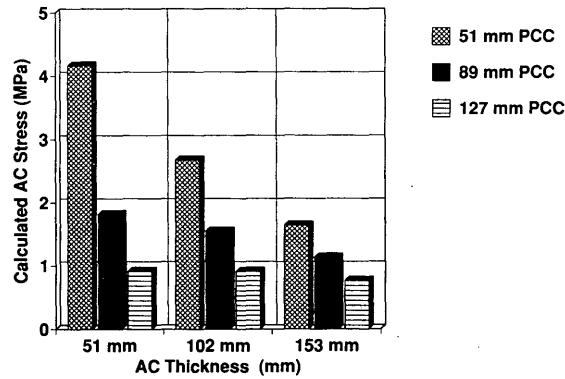


**FIGURE 9** Calculated AC stresses for various AC and PCC thicknesses.

equivalent thickness. Although Odemark (8), Packard (9), and Ioannides et al. (10) have proposed similar concepts for other types of pavement systems, we believe that this concept has never been used to specifically address concrete bonded to underlying AC layers.

### Slab Studies

The slabs built in Louisville [ $0.61 \times 0.61$  m ( $2 \times 2$  ft)] were also modeled using the finite element program ILLI-SLAB. In this model, the mesh for the 1.83-m (6-ft) edge slabs was used with joints added at 610 mm (24 in.) and 1220 mm (48 in.). No interior or corner loadings were modeled because, at any wheel placement, an edge would be only a couple of inches away. Load transfer between the panels was modeled at 100, 80, 40, and 0 percent. Although it was not measured at Louisville, the load transfer is believed to be low because the 25.4-mm- (1-in.-) deep joint saw cuts in the 51-mm (2-in.) overlay left only a nominal amount of concrete for aggregate interlock. Interface conditions were modeled as bonded and unbonded. Even though at Louisville only the 51-mm (2.0-in.) overlay was cut into 0.61-m (2-ft) sections, both the 51-mm (2.0-in.) and 89-mm (3.5-in.) pavements were modeled in ILLI-SLAB. Figures 10 and 11 give the stresses and deflections for both the unbonded and bonded systems for 0 percent load transfer efficiency.

Figure 10 again shows the considerable effect bond has on stress. By bonding the layers, the computed flexural stresses decrease from about 7.16 MPa (1,039 lb/in.<sup>2</sup>) to about 1.03 MPa (149 lb/in.<sup>2</sup>) for the 51-mm (2.0-in.) section and from about 3.69 MPa (535 lb/in.<sup>2</sup>) to 1.29 MPa (187 lb/in.<sup>2</sup>) for the 89-mm (3.5-in.) section. Plots using other load transfer efficiencies would show similar results. Again, it is interesting to note that the stresses in the 51-mm (2.0-in.) bonded overlay are lower than the stresses in the 89-mm (3.5-in.) bonded overlay. Although not tested, it is again assumed that at some thickness, stress will start to decrease with thickness. Notice that even though the bonding decreased the stresses in the 89-mm (3.5-in.) section, the stresses in the unbonded system are still low and well within the limits of a normal concrete

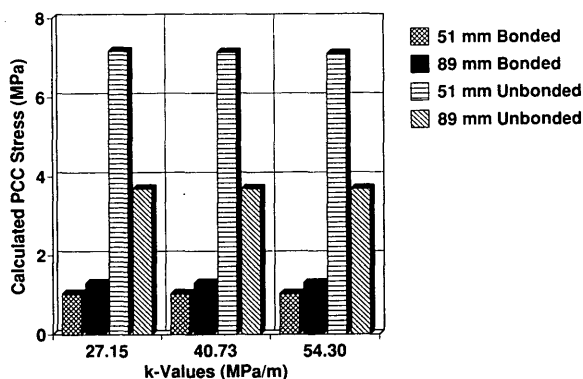


FIGURE 10 Calculated edge stresses for 0.61-m panels with 0 percent load transfer.

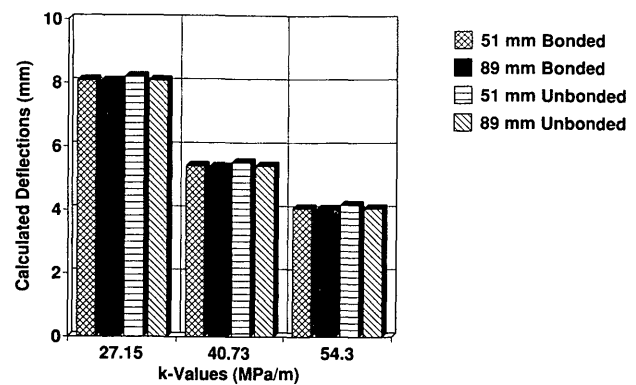


FIGURE 11 Calculated deflections for 0.61-m panels for 0 percent load transfer.

pavement. Understanding this, it should be recognized that small slab sizes may be used to counteract any possible debonding that may occur between the concrete and the AC.

Figure 11 shows the effect bond has on deflections. As with the 1.83-m (6-ft) panels, bond does not have as great an effect on deflections, and in both bonded and unbonded systems deflections are high. Again, it was found that subgrade support had a much larger impact on the deflections.

### COMPARISON WITH THE LOUISVILLE PROJECT

After 28 days and approximately 43,000 80-kN (18-kip) ESAL's, the project in Louisville has shown only a small amount of distress. About 6 percent of the slabs have shown visible signs of cracking, which was mainly concentrated at the corners of 1.83-  $\times$  1.83 m (6-  $\times$  6-ft) panels. Less than 0.6 percent of the overlay had transverse cracking. The one section of the 1.83-m (6-ft) panels that had longitudinal cracking occurred at a location that inadvertently had the entire AC layer removed during the milling process—that is, the concrete was sitting on a granular base. As of 28 days, no distresses were noted in the 0.61-m (2-ft) panels. In fact there were still no cracks in the 0.61-m (2-ft) panels after 1 year of use and over 500,000 80-kN (18-kip) ESALs (4).

It is believed that the corner cracking in the 1.83-m (6-ft) panels is the result of two actions: (a) the upturning of the corners mainly from moisture warping and (b) the high deflections at the corner. It is believed that the combination of moisture warping and high corner deflections is causing the bond between the AC and concrete to fail. Then as the corners are loaded the slab cracks as a result of the high induced concrete stresses.

Originally, it was thought that both temperature and moisture could be causing the upturning of the corners. However, using Bradbury's (11) equations to determine interior and edge curling stresses and the maximum temperature differential between the top and the bottom of the slab taken during the first 72 hr of pavement life [ $2.2^{\circ}\text{C}$  ( $4^{\circ}\text{F}$ ) for the 88.9-mm (3.5-in.) overlay], it was found that the maximum interior curling stress would be 0.145 MPa (20.96 lb/in.<sup>2</sup>) and 0.147 MPa (21.23 lb/in.<sup>2</sup>) for the 51-mm (2.0-in.) and 89-mm (3.5-

in.) pavements, respectively, whereas the maximum edge curling stress would be 0.246 MPa (35.63 lb/in.<sup>2</sup>) and 0.430 MPa (62.34 lb/in.<sup>2</sup>), respectively. Meanwhile, moisture studies by Janssen (12) from the University of Washington and Stark (13) from Construction Technologies Laboratories have shown that drying occurs in the top 12 mm (0.5 in.) of the pavement, and this drying has been calculated to cause moisture warping stresses as high as 5.52 MPa (800 lb/in.<sup>2</sup>) for a 203-mm- (8-in.-) thick pavement. Such high moisture warping stresses could cause debonding of the slab and would have a significant effect on slab dimensioning and pavement performance. Clearly this area needs more research.

## CONCLUSIONS AND RECOMMENDATIONS

This paper presented an analytical and theoretical study of the performance of a thin concrete overlay on asphalt concrete pavement built in Louisville, Kentucky. In this investigation, it was concluded that bond was critical to the pavement's performance. If bond did not exist, this pavement would fail. The second item found to be critical was the location of the neutral axis of the bonded system compared with the bottom of the concrete slab. Factors affecting the neutral axis location are concrete and AC thickness. Although this aspect was not investigated, it is believed that the modulus values of the concrete and AC will also have a critical effect on neutral axis location, which may be significant because of the temperature dependence of the AC modulus ( $E_{ac}$ ). Also found to be influential on stresses and deflections were the subgrade support conditions. Although it did not greatly affect stresses, increased subgrade support did have a large effect on deflections.

If design procedures for thin concrete overlays on AC pavements are to be developed, they must recognize that the flexural stresses in the thin concrete overlay are not the only critical item. AC radial strain and panel deflections must also be checked to ensure that they are within allowable limits. Clearly, design criteria need to be developed for AC strain and deflection, which requires much more research. Other important items for research include, but are not limited to, slab size effects and jointing requirements, bond strength and durability, concrete and AC thickness and modulus (rigidity) requirements, interaction with neighboring slabs, moisture warping and temperature curling, permanent deformation characteristics in the AC and subgrade, fatigue effects in AC and PCC and at the PCC/AC interface, and load magnitude and tire effects.

## ACKNOWLEDGMENTS

This project was sponsored by the Portland Cement Association, the American Concrete Pavement Association, and over 40 other allied industry groups and companies. The authors would like to thank all those who supported this experiment.

## REFERENCES

1. L. W. Cole and J. P. Mohsen. Construction and Instrumentation of a Thin Concrete Overlay of Asphalt Pavement. Presented at the American Concrete Institute Spring Meeting, Washington, D.C., March 1992.
2. A. J. Bush and D. R. Alexander. Pavement Evaluation Using Deflection Basin Measurements and Layered Theory. In *Transportation Research Record 1022*, TRB, National Research Council, Washington, D.C., 1985, pp. 16-29.
3. A. M. Ioannides. Dimensional Analysis in NDT Rigid Pavement Evaluation. *ASCE Journal of Transportation Engineering*, Vol. 116, No. 1, Jan. 1990, pp. 23-36.
4. High Strength Whitetopping Performance Evaluation. Preliminary Final Report. Portland Cement Association, July 1992.
5. A. M. Ioannides, M. R. Thompson, and E. J. Barenberg. Westergaard Solutions Reconsidered. *Transportation Research Record 1043*, TRB, National Research Council, Washington D.C., 1985.
6. A. M. Tabatabaie-Raissi. *Structural Analysis of Concrete Pavement Joints*. Ph.D. thesis. University of Illinois, Urbana, 1977.
7. A. M. Ioannides, M. R. Thompson, and E. J. Barenberg. Analysis of Slabs-on-Grade Pavement Systems Using a Variety of Support Models. *Proc. 3rd International Conference on Concrete Pavement Design and Rehabilitation*, Purdue University, April 23-25, 1985, pp. 309-324.
8. N. Odemark. *Investigation of the Elastic Properties of Different Soil Types and Theory for Calculation of Pavements According to the Theory of Elasticity*. Bulletin 77, State Highway Commission, Stockholm, Sweden, 1949.
9. Robert G. Packard. Structural Design of Concrete Pavements with Lean Concrete Lower Course. *Proc., 2nd International Conference on Concrete Pavement Design and Rehabilitation*, Purdue University, April 14-16, 1981, pp. 119-131.
10. A. M. Ioannides, L. Khazanovich, and J. L. Becque. Structural Evaluation of Base Layers in Concrete Pavement Systems. Presented at 71st Annual Meeting of the Transportation Research Board, Washington, D.C., 1991.
11. R. D. Bradbury. *Reinforced Concrete Pavements*. Wire Reinforcement Institute, Washington, D.C., 1938.
12. D. J. Janssen. Moisture in Portland Cement Concrete. In *Transportation Research Record 1121*, TRB National Research Council, Washington D.C., 1987.
13. D. C. Stark. Moisture Condition of Field Concrete Exhibiting Alkali-Silica Reactivity. *Proc., 2nd CANMET/ACI International Conference on Durability of Concrete*, Montreal, Quebec, Canada, 1991.

Publication of this paper sponsored by Committee on Pavement Rehabilitation.